Boundary element method with high order impedance boundary condition in electromagnetism

Christian Daveau, Abil Aubakirov, Soumaya Oueslati

Boundary element method with high order impedance boundary condition in electromagnetism

Christian Daveau *,[1], Abil Aubakirov †,[1], and Soumaya Oueslati‡,[1]

[1]Department of Mathematics, CNRS(UMR 8088), CY Cergy Paris University, 2 avenue Adolphe Chauvin, 95302 Cergy-Pontoise, France

Abstract

The present paper introduces a surface formulation to solve the scattering problem for coated objects using the integral method and a high order impedance boundary condition (HOIBC). We study the existence and uniqueness of the solution, and we propose a discretization of this formulation trough Rao-Wilton-Glisson functions (RWG). Numerical results are obtained with a 3D MoM code running on MPI clusters. The experiments show how the HOIBC significantly improves the accuracy of the results compared to computations using the standard impedance boundary condition (SIBC).
Keywords: boundary element method, scattering problem, Lagrange multipliers, high order impedance boundary condition.
AMS Subject Classification: 65R20, 65N38, 32A55

1 Introduction

The goal of this work is to solve time-harmonic scattering problem using an integral method coupled with an impedance boundary condition. Generally, the impedance boundary is considered to be constant, which is called Leontovitch or standard impedance boundary condition (see for example [2, 27, 20, 14]). This method is widely used in computational electromagnetic methods to model thin coatings on perfectly conducting objects since it drastically reduces the number of unknowns. It is recognized that this type of boundary condition can be advantageously used to get a more tractable problem in numerous complex situations of electromagnetic scattering computations (see for example [1, 30, 8, 20, 14, 29]).

In this framework, some approximations of the HOIBC are proposed in [10, 19, 20] which involve at most a first derivative of the field. Other strategies have also been established in [25, 3] that based on a polynomial approximation of the impedance operator is done in the spectral domain. The impedance boundary condition is a function

*christian.daveau@cyu.fr
†abil.aubakirov@cyu.fr
‡soumaya.oueslati1@cyu.fr

of incidence angle and polarization. There exists other papers about the approximate boundary condition in electromagnetism (see for example [29, 4, 5, 6, 7, 8, 23]).

In this paper, we consider the problem of electromagnetic scattering for a perfect conducting body with a complex coating for an incident electromagnetic field $(\mathbf{E}, \mathbf{H})$. Let Ω be a bounded domain with a Lipschitz-continuous boundary Γ. Let n be the unit normal vector to Γ directed to the exterior of Ω. We define Ω_+ as the space of radiating electric fields $\mathbf{E}$ solutions of Maxwell equations. Waves propagate with a constant wave number k in the exterior unbounded domain Ω. The electric field $\mathbf{E}$ satisfies the harmonic Maxwell equation

$$\nabla \times (\nabla \times \mathbf{E}) - k^2 \mathbf{E} = 0$$

while the related magnetic field is given by

$$\mathbf{H} = \frac{1}{ik} \nabla \times \mathbf{E}$$

An electric field is said to be radiating if it satisfies the Silver-Müller radiation condition [9, 11]:

$$\lim_{r \to \infty} r(\mathbf{E} \times \mathbf{n}_r + \mathbf{H}) = 0,$$

where $r = |\mathbf{x}|$ and $\mathbf{n}_r = \dfrac{\mathbf{x}}{|\mathbf{x}|}$, $\mathbf{x} \in \mathbb{R}^3$.
The coating is modeled by the following impedance boundary condition:

$$\mathbf{E}_t - Z(n \times \mathbf{H}) = 0 \quad on \quad \Gamma. \tag{1}$$

Here, Z is the impedance operator that depends on the incident angle, and $\mathbf{E}_t$ denotes the tangent component on the surface defined as:

$$\mathbf{E}_t = n \times (\mathbf{E} \times n).$$

An approximation of this impedance operator is given in the Section 2.1. It depends on the layer thickness, the dielectric characteristics of the layer medium, as well as on the incident angle of the electromagnetic plane wave. Our problem writes as follows:

$$\begin{cases} \nabla \times (\nabla \times \mathbf{E}) - k^2 \mathbf{E} = 0 \quad \Omega_+, \\ \nabla \times (\nabla \times \mathbf{H}) - k^2 \mathbf{H} = 0 \quad \Omega_+, \\ \mathbf{E}_t - Z(n \times \mathbf{H}) = 0 \quad on \quad \Gamma. \\ \lim_{r \to \infty} r(\mathbf{E} \times \mathbf{n}_r + \mathbf{H}) = 0. \end{cases} \tag{2}$$

This paper deals with the implementation of high order impedance boundary condition implemented in an integral equation a 3D code using RWG basis functions.

In Section 2, we give an approximation of the impedance operator with Hodge operator, and of the impedance boundary condition. Subsequently, we derive a formulation for the three-dimensional scattering problem. Then we prove the existence and uniqueness of a solution for this variational formulation and describe its discretization. In Section 4, we present our implementation methods using the H-matrix approach with ACA compression and MPI parallelization. The numerical results are presented in Section 5. Finally, the paper concludes in Section 7.

2 Variational formulation with HOIBC

2.1 High order impedance boundary condition

The approximate boundary conditions is based on a relationship between the tangential electric and magnetic fields on the boundary between the exterior of the coated body and free space. This is a local property. In this section, we propose a new impedance boundary condition with integral operators. In [25] the authors approximated the impedance condition as a ratio of second order polynomials of the sine of the incidence angle in the spectral domain. For the case of a rotational invariant coating, they obtained a high order impedance boundary condition in spatial domain equations, which is:

$$\begin{bmatrix} 1+b_1\partial_x^2+b_2\partial_y^2 & (b_1-b_2)\partial_{xy}^2 \\ (b_1-b_2)\partial_{xy}^2 & 1+b_2\partial_x^2+b_1\partial_y^2 \end{bmatrix} \begin{pmatrix} E_x \\ E_y \end{pmatrix} = \begin{bmatrix} a_0+a_1\partial_x^2+a_2\partial_y^2 & (a_1-a_2)\partial_{xy}^2 \\ (a_1-a_2)\partial_{xy}^2 & a_0+a_2\partial_x^2+a_1\partial_y^2 \end{bmatrix} \begin{pmatrix} -H_y \\ H_x \end{pmatrix} \tag{3}$$

We apply algebraic properties on equation (3) and we get:

$$(I+b_1L_D-b_2L_R)\mathbf{E}_t = (a_0I+a_1L_D-a_2L_R)(\mathbf{n}\times\mathbf{H}). \tag{4}$$

This approximation contains the operators L_D and L_R which are defined for all vector functions $\mathbf{A}$ sufficiently smooth, such that $\mathbf{A}.\mathbf{n}=0$

$$L_D(\mathbf{A}) = \nabla_\Gamma(\mathrm{div}_\Gamma\mathbf{A}), \qquad L_R(\mathbf{A}) = \mathrm{rot}_\Gamma(\mathrm{rot}_\Gamma\mathbf{A}).$$

In [21], different methods to calculate these coefficients (a_0, a_j, b_j) for the formula (4) are presented. In the following, we aim to establish a new variational formulation, applying a boundary integral method with HOIBC for the problem in the 3D case.

2.2 Implementation of the HOIBC coupled by an integral equation

We introduce the current densities $\mathbf{J}$ and $\mathbf{M}$ on the boundary Γ as follows:

$$\mathbf{M} = \mathbf{E}\times\mathbf{n} \ \ , \ \mathbf{J} = \mathbf{n}\times\mathbf{H}.$$

Note that the HOIBC equation (4) links $\mathbf{J}$ and $\mathbf{M}$ through the following relation:

$$(I+b_1L_D-b_2L_R)(\mathbf{n}\times\mathbf{M}) = (a_0I+a_1L_D-a_2L_R)\mathbf{J}. \tag{5}$$

Now, we derive the formulation. Multiplying the equation 5 by $\mathbf{\Psi}_J$ and integrating on the surface, we obtain

$$\int_\Gamma (I+b_1L_D-b_2L_R)(\mathbf{n}\times\mathbf{M})\cdot\mathbf{\Psi}_J ds = \int_\Gamma (a_0I+a_1L_D-a_2L_R)\mathbf{J}\cdot\mathbf{\Psi}_J ds,$$

hence

$$\int_\Gamma (\mathbf{n}\times\mathbf{M})\cdot\mathbf{\Psi}_J ds = \int_\Gamma (a_0I+a_1L_D-a_2L_R)\mathbf{J}\cdot\mathbf{\Psi}_J - (b_1L_D-b_2L_R)(\mathbf{n}\times\mathbf{M})\cdot\mathbf{\Psi}_J ds. \tag{6}$$

Multiplying next the equation (5) by $\mathbf{n}\times\mathbf{\Psi}_M$ and integrating on the surface, we obtain

$$\int_\Gamma (I+b_1L_D-b_2L_R)(\mathbf{n}\times\mathbf{M})\cdot(\mathbf{n}\times\mathbf{\Psi}_M)ds=\int_\Gamma (a_0I+a_1L_D-a_2L_R)\mathbf{J}\cdot(\mathbf{n}\times\mathbf{\Psi}_M)ds,$$

hence

$$\int_\Gamma \mathbf{J}\cdot(\mathbf{n}\times\mathbf{\Psi}_M)ds=\frac{1}{a_0}\int_\Gamma (I+b_1L_D-b_2L_R)(\mathbf{n}\times\mathbf{M})\cdot(\mathbf{n}\times\mathbf{\Psi}_M)ds$$
$$-\frac{1}{a_0}\int_\Gamma (a_1L_D-a_2L_R)\mathbf{J}\cdot(\mathbf{n}\times\mathbf{\Psi}_M)ds. \tag{7}$$

In order to establish the variational formulation, we insert (6) and (7) in **EFIE** and **MFIE** respectively using the formula of vector analysis.

Since $\mathrm{rot}_\Gamma A$ and $\mathrm{div}_\Gamma(\mathbf{n}\times\mathbf{A})$ do not make sense for $\mathbf{A}\in H^{-\frac{1}{2}}(\mathrm{div},\Gamma)$, we introduce auxiliary unknowns $\tilde{\mathbf{J}}$ and $\tilde{\mathbf{M}}$ from $H^{-\frac{1}{2}}(\mathrm{div},\Gamma)$ with test functions $\tilde{\mathbf{\Psi}}_J$ and $\tilde{\mathbf{\Psi}}_M$. This method is inspired by recent papers [12, 18]. We finally obtain the following variational formulation

Problem 2.1. *Find* $U=(\mathbf{J},\mathbf{M},\tilde{\mathbf{J}},\tilde{\mathbf{M}})\in V=[H^{-1/2}(div,\Gamma)\cap L^2(\Gamma)]^4$ *and* $\lambda=(\boldsymbol{\lambda}_J,\boldsymbol{\lambda}_M)\in[H^{-1/2}(\Gamma)]^2$ *such that*

$$\begin{cases} A(U,\Psi)+B^T(\lambda,\Psi)=F(\Psi)\\ B(U,\lambda')=0\end{cases} \tag{8}$$

for all $\Psi=(\mathbf{\Psi}_J,\mathbf{\Psi}_M,\tilde{\mathbf{\Psi}}_J,\tilde{\mathbf{\Psi}}_M)\in V=[H^{-1/2}(div,\Gamma)\cap L^2(\Gamma)]^4$ *and* $\lambda'=(\boldsymbol{\lambda}'_J,\boldsymbol{\lambda}'_M)\in W=[H^{-1/2}(\Gamma)]^2$.

The bilinear forms are defined by:

$$B(U,\lambda')=\int_\Gamma \boldsymbol{\lambda}'_J\cdot(\tilde{\mathbf{J}}-\mathbf{n}\times\mathbf{J})ds+\int_\Gamma \boldsymbol{\lambda}'_M\cdot(\tilde{\mathbf{M}}-\mathbf{n}\times\mathbf{M})ds$$

and

$$A(U,\Psi)=iZ_0\iint_\Gamma kG\,(\mathbf{J}\cdot\mathbf{\Psi}_J)-\frac{1}{k}G\ \mathrm{div}\mathbf{\Psi}_J\ \mathrm{div}\mathbf{J}dsds' \tag{9}$$
$$+\frac{i}{Z_0}\iint_\Gamma kG\,(\mathbf{\Psi}_M\cdot\mathbf{M})-\frac{1}{k}G\ \mathrm{div}\mathbf{\Psi}_M\ \mathrm{div}\mathbf{M}dsds'$$
$$+\iint_\Gamma \nabla'G\cdot(\mathbf{\Psi}_J\times\mathbf{M})dsds'-i\iint_\Gamma \nabla'G\cdot(\mathbf{\Psi}_M\times\mathbf{J})dsds'$$
$$+\frac{a_0}{2}\int_\Gamma \mathbf{J}\cdot\mathbf{\Psi}_Jds+\frac{1}{2a_0}\int_\Gamma \mathbf{M}\cdot\mathbf{\Psi}_Mds$$
$$-\frac{a_1}{2}\int_\Gamma \mathrm{div}_\Gamma\mathbf{J}\ \mathrm{div}_\Gamma\mathbf{\Psi}_Jds-\frac{a_2}{2}\int_\Gamma \mathrm{div}_\Gamma\tilde{\mathbf{J}}\ \mathrm{div}_\Gamma\tilde{\mathbf{\Psi}}_Jds$$
$$+\frac{b_1}{2}\int_\Gamma \mathrm{div}_\Gamma\tilde{\mathbf{M}}\ \mathrm{div}_\Gamma\mathbf{\Psi}_Jds-\frac{b_2}{2}\int_\Gamma \mathrm{div}_\Gamma\mathbf{M}\ \mathrm{div}_\Gamma\tilde{\mathbf{\Psi}}_Jds$$
$$-\frac{b_1}{2a_0}\int_\Gamma \mathrm{div}_\Gamma\tilde{\mathbf{M}}\ \mathrm{div}_\Gamma\tilde{\mathbf{\Psi}}_Mds-\frac{b_2}{2a_0}\int_\Gamma \mathrm{div}_\Gamma\mathbf{M}\ \mathrm{div}_\Gamma\mathbf{\Psi}_Mds$$

$$+\frac{a_1}{2a_0}\int_\Gamma \mathrm{div}_\Gamma \mathbf{J}\ \mathrm{div}_\Gamma \tilde{\mathbf{\Psi}}_M ds - \frac{a_2}{2a_0}\int_\Gamma \mathrm{div}_\Gamma \tilde{\mathbf{J}}\ \mathrm{div}_\Gamma \mathbf{\Psi}_M ds,$$

where $G(x,y)$ is the Green kernel.

In the next section, we study this problem mathematically.

2.3 Existence and uniqueness theorem

We use a theorem from [13] to prove the existence and uniqueness of a solution to the problem 2.1. First, we prove the following result.

Lemma 2.1. *The operator A is continuous on $V \times V$ for all $\Psi \in V$ and we have*

$$|A(U,\Psi)| \leq C\|U\|_V \|\Psi\|_V$$

Proof. In order to prove this lemma, it is convenient to introduce a decomposition of A as $A = A_1 + A_2 + A_3$
where

$$A_1(U,\Psi) = < Z_0(B-S)\mathbf{J}, \mathbf{\Psi}_J > + \frac{1}{Z_0} < (B-S)\mathbf{M}, \mathbf{\Psi}_M >$$

$$+ < Q\mathbf{M}, \mathbf{\Psi}_J > - < Q\mathbf{J}, \mathbf{\Psi}_M > + \frac{a_0}{2} < \mathbf{J}, \mathbf{\Psi}_J > + \frac{1}{2a_0} < \mathbf{M}, \mathbf{\Psi}_M >$$

$$A_2(U,\Psi) = -\frac{a_1}{2} < \mathrm{div}_\Gamma \mathbf{J}, \mathrm{div}_\Gamma \mathbf{\Psi}_J > - \frac{a_2}{2} < \mathrm{div}_\Gamma \tilde{\mathbf{J}}, \mathrm{div}_\Gamma \tilde{\mathbf{\Psi}}_J >$$

$$- \frac{b_1}{2a_0} < \mathrm{div}_\Gamma \tilde{\mathbf{M}}, \mathrm{div}_\Gamma \tilde{\mathbf{\Psi}}_M > - \frac{b_2}{2a_0} < \mathrm{div}_\Gamma \mathbf{M}, \mathrm{div}_\Gamma \mathbf{\Psi}_M >$$

and

$$A_3(U,\Psi) = \frac{b_1}{2} < \mathrm{div}_\Gamma \tilde{\mathbf{M}}, \mathrm{div}_\Gamma \mathbf{\Psi}_J > - \frac{b_2}{2} < \mathrm{div}_\Gamma \mathbf{M}, \mathrm{div}_\Gamma \tilde{\mathbf{\Psi}}_J >$$

$$+ \frac{a_1}{2a_0} < \mathrm{div}_\Gamma \mathbf{J}, \mathrm{div}_\Gamma \tilde{\mathbf{\Psi}}_M > - \frac{a_2}{2a_0} < \mathrm{div}_\Gamma \tilde{\mathbf{J}}, \mathrm{div}_\Gamma \mathbf{\Psi}_M >$$

Hence, the theorems 2.2 and 4.6 in [14] yield that there exist constants C_1 and C_2 such that

$$|A_1(U,\Psi)| \leq C_1\|U\|_V \|\Psi\|_V, \tag{10}$$

and

$$|A_2(U,\Psi) + A_3(U,\Psi)| \leq C_2\|U\|_V \|\Psi\|_V \tag{11}$$

Combining (10) and (11) we obtain:

$$|A(U,\Psi)| = |A_1 + A_2 + A_3| \leq |A_1(U,\Psi)| + |A_2(U,\Psi) + A_3(U,\Psi)| \leq C\|U\|_V \|\Psi\|_V$$

where $C = C_1 + C_2$. □

Lemma 2.2. *The operator A is coercive on V. We have to show that there exists $\alpha > 0$ such that*

$$\Re[A(U,U^*)] \geq \alpha\|U\|_V^2 - C\|U\|_V^2, \ \forall U \in V.$$

Proof. It follow from [14] that there exists α such that

$$\Re(A_1) = \Re(< Z_0(B-S)\mathbf{J}, \mathbf{J}^* >) + \Re(< Z_0^{-1}(B-S)\mathbf{M}, \mathbf{M}^* >) + \Re(< Q\mathbf{M}, \mathbf{J}^* >)$$
$$-\Re(< Q\mathbf{J}, \mathbf{M}^* >) + \Re(\frac{a_0}{2}\int_\Gamma \mathbf{J}\cdot\mathbf{J}^* ds) + \Re(\frac{1}{2a_0}\int_\Gamma \mathbf{M}\cdot\mathbf{M}^* ds)$$
$$\geq \alpha\left(\|\mathbf{J}\|^2_{-1/2,\mathrm{div}_\Gamma} + \|\mathbf{M}\|^2_{-1/2,\mathrm{div}_\Gamma}\right) + \frac{\Re(a_0)}{2}\|\mathbf{J}\|^2_{L^2(\Gamma)} + \frac{\Re(a_0)}{2|a_0|^2}\|\mathbf{M}\|^2_{L^2(\Gamma)}.$$

We can easily show that

$$\Re(A_2) = -\frac{\Re(a_1)}{2}\|\mathrm{div}_\Gamma\mathbf{J}\|^2_{L^2(\Gamma)} - \frac{\Re(a_2)}{2}\|\mathrm{div}_\Gamma\tilde{\mathbf{J}}\|^2_{L^2(\Gamma)}$$
$$-\frac{\Re(b_1a_0^*)}{2|a_0|^2}\|\mathrm{div}_\Gamma\tilde{\mathbf{M}}\|^2_{L^2(\Gamma)} - \frac{\Re(b_2a_0^*)}{2|a_0|^2}\|\mathrm{div}_\Gamma\mathbf{M}\|^2_{L^2(\Gamma)}$$

On the other hand, we get:

$$\Re(A_3) = \Re(\frac{b_1}{2}\int_\Gamma \mathrm{div}_\Gamma\tilde{\mathbf{M}}\ \mathrm{div}_\Gamma\mathbf{J}^* ds) - \Re(\frac{b_2}{2}\int_\Gamma \mathrm{div}_\Gamma\mathbf{M}\ \mathrm{div}_\Gamma\tilde{\mathbf{J}}^* ds)$$
$$+\Re(\frac{a_1}{2a_0}\int_\Gamma \mathrm{div}_\Gamma\mathbf{J}\ \mathrm{div}_\Gamma\tilde{\mathbf{M}}^* ds) - \Re(\frac{a_2}{2a_0}\int_\Gamma \mathrm{div}_\Gamma\tilde{\mathbf{J}}\ \mathrm{div}_\Gamma\mathbf{M}^* ds)$$
$$= \Re\left\{\left(\frac{b_1}{2}+\frac{a_1^*}{2a_0^*}\right)\int_\Gamma \mathrm{div}_\Gamma\tilde{\mathbf{M}}\ \mathrm{div}_\Gamma\mathbf{J}^* ds\right\} - \Re\left\{\left(\frac{b_2}{2}+\frac{a_2^*}{2a_0^*}\right)\int_\Gamma \mathrm{div}_\Gamma\tilde{\mathbf{J}}^*\ \mathrm{div}_\Gamma\mathbf{M} ds\right\}$$
$$= \Re\left\{\int_\Gamma \frac{1}{|a_0|^{1/2}}\left(\frac{b_1}{2}+\frac{a_1^*a_0}{2|a_0|^2}\right)^{1/2}\mathrm{div}_\Gamma\tilde{\mathbf{M}}\ \cdot|a_0|^{1/2}\left(\frac{b_1}{2}+\frac{a_1^*a_0}{2|a_0|^2}\right)^{1/2}\mathrm{div}_\Gamma\mathbf{J}^* ds\right\}$$
$$-\Re\left\{\int_\Gamma |a_0|^{1/2}\left(\frac{b_2}{2}+\frac{a_2^*a_0}{2|a_0|^2}\right)^{1/2}\mathrm{div}_\Gamma\tilde{\mathbf{J}}^*\cdot\frac{1}{|a_0|^{1/2}}\left(\frac{b_2}{2}+\frac{a_2^*a_0}{2|a_0|^2}\right)^{1/2}\mathrm{div}_\Gamma\mathbf{M} ds\right\}.$$

We also define q_1 and q_2 by

$$q_1 = b_1|a_0| + a_1^*a_0/|a_0| \qquad q_2 = b_2|a_0| + a_2^*a_0/|a_0|,$$

and we find that

$$\Re(A_3) \geq -\frac{|q_1|}{4}\|\mathrm{div}_\Gamma\mathbf{J}\|^2_{L^2(\Gamma)} - \frac{|q_1|}{4|a_0|^2}\|\mathrm{div}_\Gamma\tilde{\mathbf{M}}\|^2_{L^2(\Gamma)}$$
$$-\frac{|q_2|}{4}\|\mathrm{div}_\Gamma\tilde{\mathbf{J}}\|^2_{L^2(\Gamma)} - \frac{|q_2|}{4|a_0|^2}\|\mathrm{div}_\Gamma\mathbf{M}\|^2_{L^2(\Gamma)}.$$

Using the conditions on the coefficients

$$\Re(a_j) + \frac{|q_j|}{2} = 0, \quad \text{where } j = 1,2$$

and from the sufficient uniqueness conditions, we get $\Re(a_j) = \Re(b_j^*a_0)$.
Thus, we obtain

$$\Re(A_2) + \Re(A_3) \geq 0.$$

Finally, for an operator A, we have

$$\Re(A) \geq \alpha\left(\|\mathbf{J}\|^2_{-1/2,\mathrm{div}_\Gamma} + \|\mathbf{M}\|^2_{-1/2,\mathrm{div}_\Gamma}\right) + \frac{\Re(a_0)}{2}\|\mathbf{J}\|^2_{L^2(\Gamma)} + \frac{\Re(a_0)}{2|a_0|^2}\|\mathbf{M}\|^2_{L^2(\Gamma)}$$

□

Lemma 2.3. *The operator B verifies the inequality*

$$\sup_{\|U\|_V=1} |B(U,\lambda)| \geq \beta \|\lambda\|_W, \ \forall \lambda \in W = [H^{-1/2}(\Gamma)]^3 \times [H^{-1/2}(\Gamma)]^3$$

where $U \in V = [H^{-1/2}(div,\Gamma) \cap L^2(\Gamma)]^4$ and $\beta > 0$.

Proof. We have to show that there exists $\beta > 0$ such that

$$\sup_{\|U\|_V=1} \left| \int_\Gamma \boldsymbol{\lambda}_J \cdot (\tilde{\mathbf{J}} - n \times \mathbf{J}) + \boldsymbol{\lambda}_M \cdot (\tilde{\mathbf{M}} - n \times \mathbf{M}) ds \right| \geq \beta \|\lambda\|_W$$

First, we take

$$\mathbf{J} = 0; \ \mathbf{M} = 0; \ \tilde{\mathbf{J}} = \frac{\hat{\mathbf{J}}}{\|\hat{\mathbf{J}}\|_V} \ \ and \ \ \tilde{\mathbf{M}} = \frac{\hat{\mathbf{M}}}{\|\hat{\mathbf{M}}\|_V}$$

$$\hat{\mathbf{J}}(x) = \int_{\Gamma \setminus x} \frac{\boldsymbol{\lambda}_J}{|x-y|} ds_y \quad and \quad \hat{\mathbf{M}}(y) = \int_{\Gamma \setminus x} \frac{\boldsymbol{\lambda}_M}{|x-y|} ds_y$$

so, we get following inequality:

$$\sup_{\|U\|_V=1} \left| \int_\Gamma \boldsymbol{\lambda}_J \cdot (\tilde{\mathbf{J}} - n \times \mathbf{J}) + \boldsymbol{\lambda}_M \cdot (\tilde{\mathbf{M}} - n \times \mathbf{M}) ds \right| \geq$$

$$\frac{1}{\|\hat{\mathbf{J}}\|_{-1/2,\mathrm{div}_\Gamma}} \iint_\Gamma \frac{\boldsymbol{\lambda}_J(x)\boldsymbol{\lambda}_J(y)}{|x-y|} ds_y ds_x + \frac{1}{\|\hat{\mathbf{M}}\|_{-1/2,\mathrm{div}_\Gamma}} \iint_\Gamma \frac{\boldsymbol{\lambda}_M(x)\boldsymbol{\lambda}_M(y)}{|x-y|} ds_y ds_x \quad (12)$$

Using the Planchard-Nédélec inequality [15], we get

$$\iint_\Gamma \frac{\lambda(x)\lambda(y)}{|x-y|} ds_y ds_x \geq \beta \|\lambda\|^2_{-1/2,\Gamma} \quad (13)$$

and therefore, by (12) and (13), it follows that

$$\sup_{\|U\|_V=1} \left| \int_\Gamma \boldsymbol{\lambda}_J \cdot (\tilde{\mathbf{J}} - n \times \mathbf{J}) + \boldsymbol{\lambda}_M \cdot (\tilde{\mathbf{M}} - n \times \mathbf{M}) ds \right| \geq$$

$$\frac{1}{\|\hat{\mathbf{J}}\|_{-1/2,\mathrm{div}_\Gamma}} \beta_J \|\lambda_J\|^2_{-1/2,\Gamma} + \frac{1}{\|\hat{\mathbf{M}}\|_{-1/2,\mathrm{div}_\Gamma}} \beta_M \|\lambda_M\|^2_{-1/2,\Gamma} \quad (14)$$

Furthermore, there exist $C_J > 0$ and $C_M > 0$ such that

$$\|\hat{\mathbf{J}}\|_{-1/2,\mathrm{div}_\Gamma} \leq C_J \|\lambda_J\|_{-1/2,\Gamma} \ \ and \ \ \|\hat{\mathbf{M}}\|_{-1/2,\mathrm{div}_\Gamma} \leq C_M \|\lambda_M\|_{-1/2,\Gamma} \quad (15)$$

Consequently, we obtain that

$$\begin{aligned} \sup_{\|U\|_V=1} \left| \int_\Gamma \boldsymbol{\lambda}_J \cdot (\tilde{\mathbf{J}} - n \times \mathbf{J}) + \boldsymbol{\lambda}_M \cdot (\tilde{\mathbf{M}} - n \times \mathbf{M}) ds \right| &\geq \frac{\beta_J}{C_J} \|\lambda_J\|_{-1/2,\Gamma} + \frac{\beta_M}{C_M} \|\lambda_M\|_{-1/2,\Gamma} \\ &\geq \beta \|\lambda\|_W \end{aligned}$$

where $\beta = \min(\beta_J/C_J; \beta_M/C_M)$. □

Theorem 2.1. *The problem (2.1) admits a unique solution* $U \in V = [H^{-1/2}(div, \Gamma) \cap L^2(\Gamma)]^4$ *and* $\lambda \in [H^{-1/2}(\Gamma)]^2$*, if the coefficients satisfy*

$$\Re(a_j) + \frac{|a_0||b_j + a_j^*/a_0^*|}{2} = 0 \quad for \quad j = 1, 2. \tag{16}$$

Proof. Using the above lemma, we can show as in [13] that the variational problem 2.1 has a unique solution. □

In the next section, a discretization of the problem 2.1 is obtained using Rao-Wilton functions.

3 Discretization of the variational problem with HOIBC

As a next step, we express the problem in matrix form. Let $\{\mathbf{f}_i\}_{i=1,N_e}$ be a set of Rao-Wilton-Glisson functions [16, 17]. We decompose the electric and magnetic currents with these basis functions. For the Lagrange multipliers, we use the basis functions $\mathbf{g}_n$ proposed in [12]. We obtain these following integrals:

$$(B-S)_{i,j} = i \int\int_{\Gamma_h} kG(s,s')\mathbf{f}_j(s') \cdot \mathbf{f}_i(s) - \frac{1}{k} G(s,s')(\mathbf{div}_\Gamma \mathbf{f}_i)(\mathbf{div}'_\Gamma \mathbf{f}_j) ds ds'$$

$$Q_{i,j} = -i \int\int_{\Gamma_h} [\mathbf{f}_i(s) \times \mathbf{f}_j(s')] \cdot \nabla'_\Gamma G(s,s') ds ds'$$

$$I_{i,j} = \int_{\Gamma_h} \mathbf{f}_i \cdot \mathbf{f}_j ds; \quad D_{i,j} = \int_{\Gamma_h} (\mathbf{div}_\Gamma \mathbf{f}_j)(\mathbf{div}_\Gamma \mathbf{f}_i) ds$$

$$C_{Hi,j} = \int_{\Gamma_h} \mathbf{g}_i \cdot \mathbf{f}_j ds; \quad C_{Ki,j} = \int_{\Gamma_h} \mathbf{g}_i \cdot (\mathbf{n} \times \mathbf{f}_j) ds, \tag{17}$$

where $[C_H]$ is a non singular diagonal matrix. Therefore, $[C_H]$ is invertible.
Then, we define $[A1]$ and $[A2]$ by

$$[A1] = [(B-S)] + \frac{a_0}{2}[I] - \frac{a_1}{2}[D], \quad [A2] = [(B-S)] + \frac{1}{2a_0}[I] - \frac{b_2}{2a_0}[D]. \tag{18}$$

Using (17) and (18), we now present the discrete problem 2.1 in the following matrix form

$$\begin{pmatrix} [A1] & [Q] & 0 & \frac{b_1}{2}[D] & [C_K]^T & 0 \\ [Q]^T & [A2] & -\frac{a_2}{2a_0}[D] & 0 & 0 & [C_K]^T \\ 0 & -\frac{b_2}{2}[D] & -\frac{a_2}{2}[D] & 0 & [C_H]^T & 0 \\ \frac{a_1}{2a_0}[D] & 0 & 0 & -\frac{b_1}{2a_0}[D] & 0 & [C_H]^T \\ [C_K] & 0 & [C_H] & 0 & 0 & 0 \\ 0 & [C_K] & 0 & [C_H] & 0 & 0 \end{pmatrix} \begin{pmatrix} \overline{J} \\ \overline{M} \\ \overline{\tilde{J}} \\ \overline{\tilde{M}} \\ \overline{\lambda_J} \\ \overline{\lambda_M} \end{pmatrix} = \begin{pmatrix} \overline{E} \\ \overline{H} \\ 0 \\ 0 \\ 0 \\ 0 \end{pmatrix} \tag{19}$$

where right-side vectors $\overline{E}$, $\overline{H}$ are defined as follows:

$$E_i = \int_{\Gamma_h} \mathbf{E}^{inc} \cdot \mathbf{f}_i ds; \quad H_i = \int_{\Gamma_h} \mathbf{H}^{inc} \cdot \mathbf{f}_i ds.$$

As a second step, we focus on eliminating auxiliary currents and the Lagrange multiplier.

Using the definition of the basis function, we obtain

$$\int_\Gamma \mathbf{g}_n(s)\cdot\tilde{\mathbf{J}}ds = \frac{|T_n^+|+|T_n^-|}{3}\tilde{J}_n.$$

On the other side, we have

$$\int_\Gamma \mathbf{g}_n(s)\cdot(\mathbf{n}\times\mathbf{J})ds = \int_{T_n^+\cup T_n^-}\mathbf{g}_n(s)\cdot(\mathbf{n}\times\mathbf{J})ds,$$

which is calculated with help of Gaussian quadrature. We get the equation

$$\frac{|T_n^+|+|T_n^-|}{3}\tilde{J}_n = \int_{T_n^+\cup T_n^-}\mathbf{g}_n(s)\cdot(\mathbf{n}\times\mathbf{J})ds \tag{20}$$

Thus, we obtain

$$\tilde{J}_n = \frac{3}{|T_n^+|+|T_n^-|}\int_{T_n^+\cup T_n^-}\mathbf{g}_n(s)\cdot(\mathbf{n}\times\mathbf{J})ds \tag{21}$$

on each edge of the mesh. Consequently, we conclude that the auxiliary currents can be rewritten as

$$\overline{\tilde{J}} = -[C_H]^{-1}[C_K]\overline{J} \quad \text{and} \quad \overline{\tilde{M}} = -[C_H]^{-1}[C_K]\overline{M} \tag{22}$$

As a consequence, equation (19) together with (22) yields the following expression of Lagrange multipliers in terms of $\overline{J}$ and $\overline{M}$:

$$\overline{\lambda_J} = \frac{b_2}{2}[C_H]^{-T}[D]\overline{M} - \frac{a_2}{2}[C_H]^{-T}[D][C_H]^{-1}[C_K]\overline{J} \tag{23}$$

$$\overline{\lambda_M} = -\frac{a_2}{2a_0}[C_H]^{-T}[D]\overline{J} - \frac{b_1}{2a_0}[C_H]^{-T}[D][C_H]^{-1}[C_K]\overline{M} \tag{24}$$

Now we define the matrices

$$[C_{KH}] = [C_H]^{-1}[C_K] \quad \text{and} \quad [C_{KH}]^T = [C_K]^T[C_H]^{-T} \tag{25}$$

Using (23),(24) and (25), we obtain the final matrix

$$\mathcal{M}_{HOIBC} = \begin{pmatrix} [A1] - \frac{a_2}{2}[C_{KH}]^T[D][C_{KH}] & [Q] - \frac{b_1}{2}[D][C_{KH}] + \frac{b_2}{2}[C_{KH}]^T[D] \\ [Q]^T + \frac{a_2}{2a_0}[D][C_{KH}] - \frac{a_1}{2a_0}[C_{KH}]^T[D] & [A2] - \frac{b_1}{2a_0}[C_{KH}]^T[D][C_{KH}] \end{pmatrix}$$

4 Implementation methods

Considering a surface with N edges, the matrix of the HOIBC defined in the previous section is of size 2Nx2N in its dense form. This $O(N^2)$ complexity poses significant challenges in terms of memory footprint and computational costs. The current section describes the methods applied with a view to meeting both challenges via memory compression and parallel computing. We implemented these methods through an adapted version of the open-source HACApK library for CPU clusters [34, 35] which is originally designed for real-valued BEM-matrices only.

4.1 H-matrix

Hierarchical matrices or H-matrices [32, 33] are a well-known approach which allows creating a subdivided and data-sparse representation of dense BEM-matrices. The principle consists in partitioning the matrix into sub matrices called blocks, and to perform low-rank approximations of certain blocks by using an admissibility condition. The tree-based subdivision of the H-matrix is achieved by a recursive subdivision of the geometry defining groups of edges, and by permuting the indices in the matrix such that consecutive rows and columns correspond to edges at a close distance. The diagonal blocks, which represent intra-group interactions, as well as blocks of degenerated form having few rows or columns are not admissible for compression and are processed in dense mode. All other blocks correspond to interactions of well-separated groups of edges and will be compressed by the ACA algorithm which is presented in the next subsection. As an example, Figure 1 displays a typical H-matrix partitioning pattern with its admissible and non-admissible blocks.

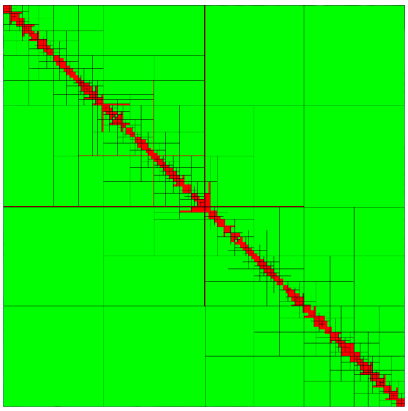

Figure 1: H-matrix partition of a sphere mesh with 1434 edges. Matrix size is 2868x2868. Admissible blocks are shown in green, non-admissible blocks in red.

4.2 Adaptive Cross Approximation

Adaptive Cross Approximation (ACA) is a greedy compression algorithm producing low-rank approximations of the admissible blocks [36]. The advantages of the ACA compared to other compression methods lie notably in the facts that (1) it is purely algebraic, i.e its formulation is integral equation kernel independent, and (2) it does not require the assembly of the complete matrix.

Every matrix of rank r is the sum of r matrices of rank 1. With this insight in mind, the ACA improves the accuracy of the approximation by successively adding rank-1 matrices. At iteration k, a block $A \in \mathbb{C}^{m*n}$ is approximated by the rank-k matrix

$$B_k = \sum_{l=1}^{k} u_l v_l^T \in U_k V_k^T, U_k \in \mathbb{C}^{m*k}, V_k \in \mathbb{C}^{n*k} \tag{26}$$

The algorithm terminates when a required accuracy is achieved, i.e. when the residual $||A - B_k||_F \leq \varepsilon ||A||_F$ for a specified tolerance ε, $||.||_F$ denoting the Frobenius norm. A block which has been compressed with rank r needs a memory space of only $r(m+n)$

entries instead of mn entries. Note that for some admissible blocks ACA may yield unprofitable compressions with $r(m+n) > mn$. In that case, we reject the compression and fall back to dense mode. A detailed description of the ACA algorithm can be found in [37].

4.3 Parallel computing

Due to the independence of the blocks, H-matrix computing can be conveniently coupled with parallel computing technologies to distribute the memory load, and to accelerate not only the matrix filling but also the classical matrix/vector product in order to obtain fast iterative solvers.

The HACApK library provides a powerful hybrid programming framework for CPU clusters with both MPI and OpenMP parallelizations. After the H-matrix partitioning into blocks, the blocks are evenly assigned to the MPI processes and filled in parallel, in dense or ACA-compressed mode depending on their admissibility. The filling is further accelerated through OpenMP directives such that multiple threads can work on different blocks at the same time.

After the filling stage, the H-matrix memory load has therefore been scattered over the MPI processes, each process holding a share of the blocks. Subsequently usual linear algebra operations can be performed. Most importantly, when the iterative solver requires a matrix/vector product, each MPI process multiplies its particular blocks with the vector and produces a partial result. The operation is again accelerated through OpenMP multithreading such that several blocks can be handled in parallel. The partial multiplications are broadcasted among the MPI processes and added up to the final product.

5 Numerical results

We present some numerical results which validate the approximation HOIBC by comparing the calculated radar coross section and a method of moments solution for several geometries that have been generated with CAPITOLE. The main goals of this section are to illustrate the numerical performance of the higher order impedance boundary condition. The following test examples are selected:

5.1 Coated sphere

As a first example, we consider the case of a coated conducting sphere with a conductor radius of $1.5\lambda_0$ and a coating thickness of $0.075\lambda_0$, with $\varepsilon_r = 5$ and $\mu_r = 1.0$. The geometry is illustrated in Figure 2.

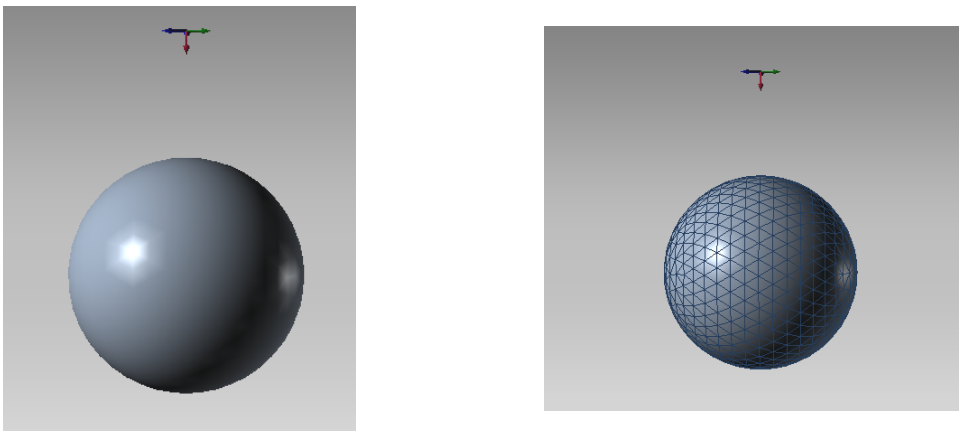

Figure 2: A mesh (right) and corresponding sphere (left).

Figure 3 shows the $\theta\theta$ components of the bistatic RCS for a plane wave incident from the angle $\theta = 0$. Three solutions are included: the exact solution (MIE) and the solutions using the method of moments with SIBC and the HOIBC. The Figure clearly illustrates the increased accuracy of the HOIBC solution compared to the SIBC solution. The SIBC only gives the average behavior of the scattered field, whereas the HOIBC accurately predicts the sidelobe behavior. In this example, the code only take the default optimization of the machine, that is , they are not parallel code.

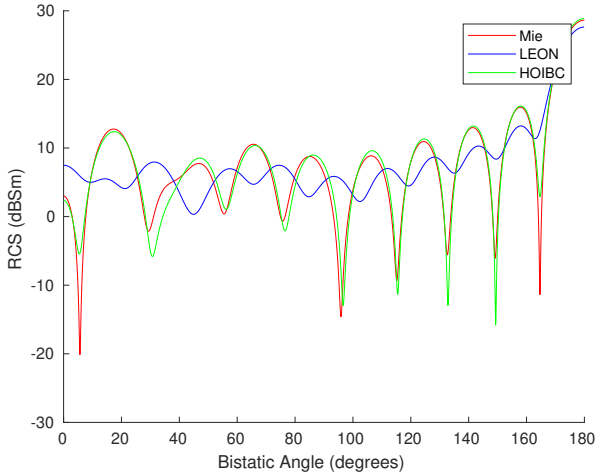

Figure 3: $\theta\theta$ component of the bistatic RCS for a coated conducting sphere. Exact serie solution and HOIBC solution.

5.2 Coated spheroïd

The second test concerns a coated conducting spheroïd whose radii are 0.5m and 1m with a coating thickness of $0.17\lambda_0$, $\varepsilon_r = 5$ and $\mu_r = 1$. The geometry is illustrated in Figure 4.

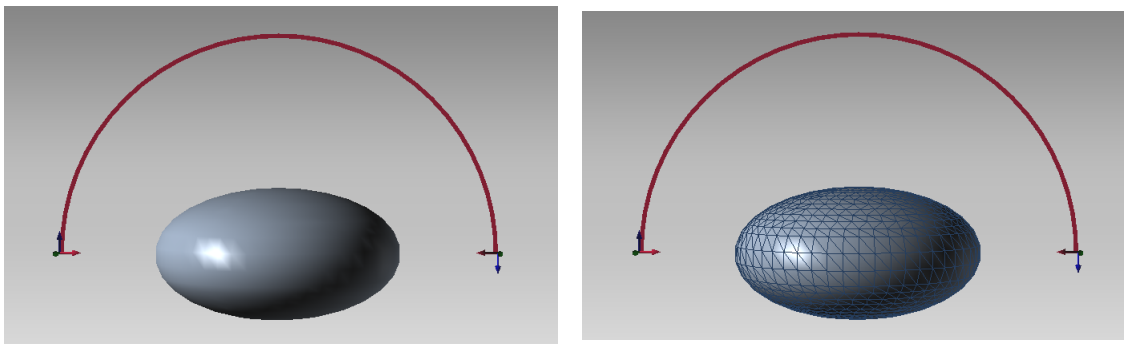

Figure 4: A mesh (right) and corresponding spheroïd (left).

Figure 5 and Figure 6 show the $\theta\theta$ and $\phi\phi$ components of the monostatic RCS. Three solutions are included : a method of moments solution called PMCHWT [24], the HOIBC solution and the SIBC solution. Note that there exists no exact solution for this case. We see only a slight difference between the PMCHWT solutions and the HOIBC solutions, whereas the SIBC solutions are very poor. In both cases excellent results are obtained with HOIBC for all angles of incidence, however the finite radii of curvature on the spheroïd contribute to the inaccuracy of the HOIBC result.

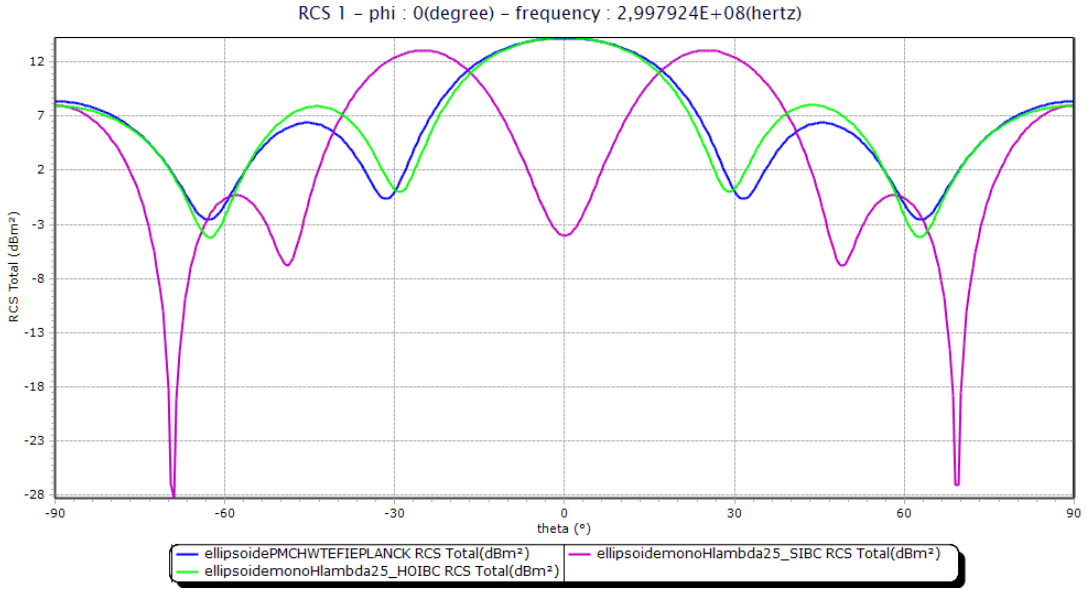

Figure 5: $\theta\theta$ component of the monostatic RCS for a coated conducting spheroïd, PMCHWT solution, SIBC solution and HOIBC solution.

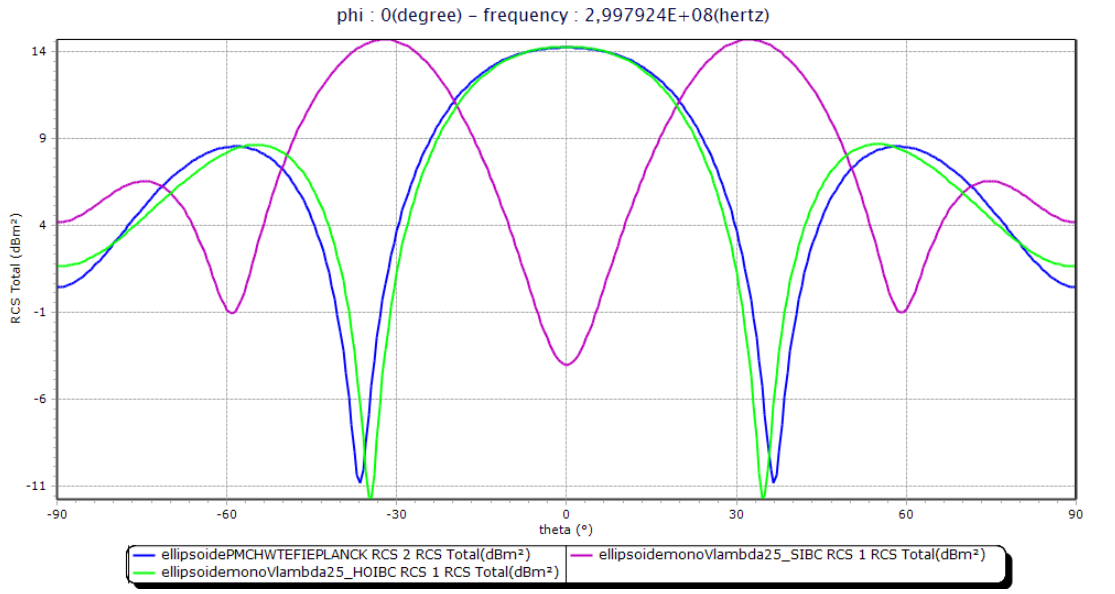

Figure 6: $\phi\phi$ component of the monostatic RCS for a coated conducting spheroïd, PMCHWT solution, SIBC solution and HOIBC solution.

5.3 Coated conesphere

The next three examples are used to illustrate the effects of the HOIBC solution. We consider the case of a coated conducting conesphere which is illustrated in Figure 7. This PEC conesphere with a half angle 15Âř and half total length 1.29 mm is coated with a 5 mm layer, coating thickness of $0.11\lambda_0$,$\epsilon_r = 5$ and $\mu_r = 1$.

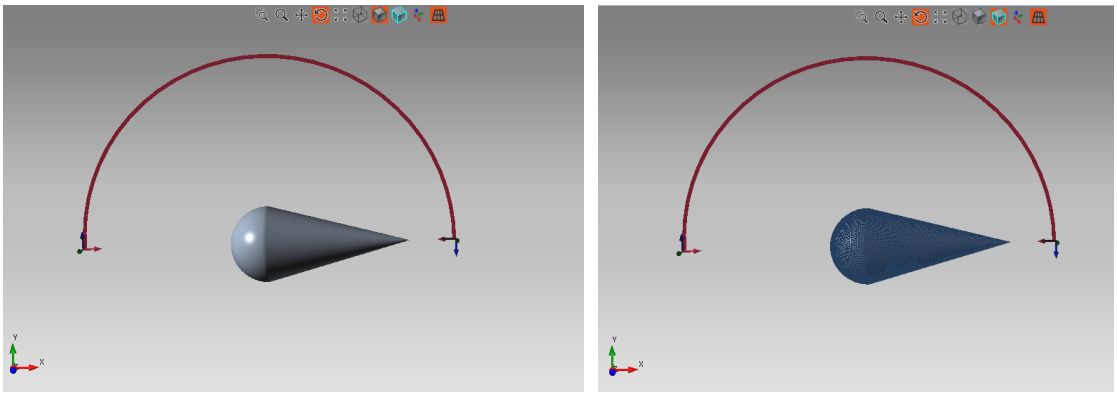

Figure 7: A mesh (right) and corresponding cone-sphere (left).

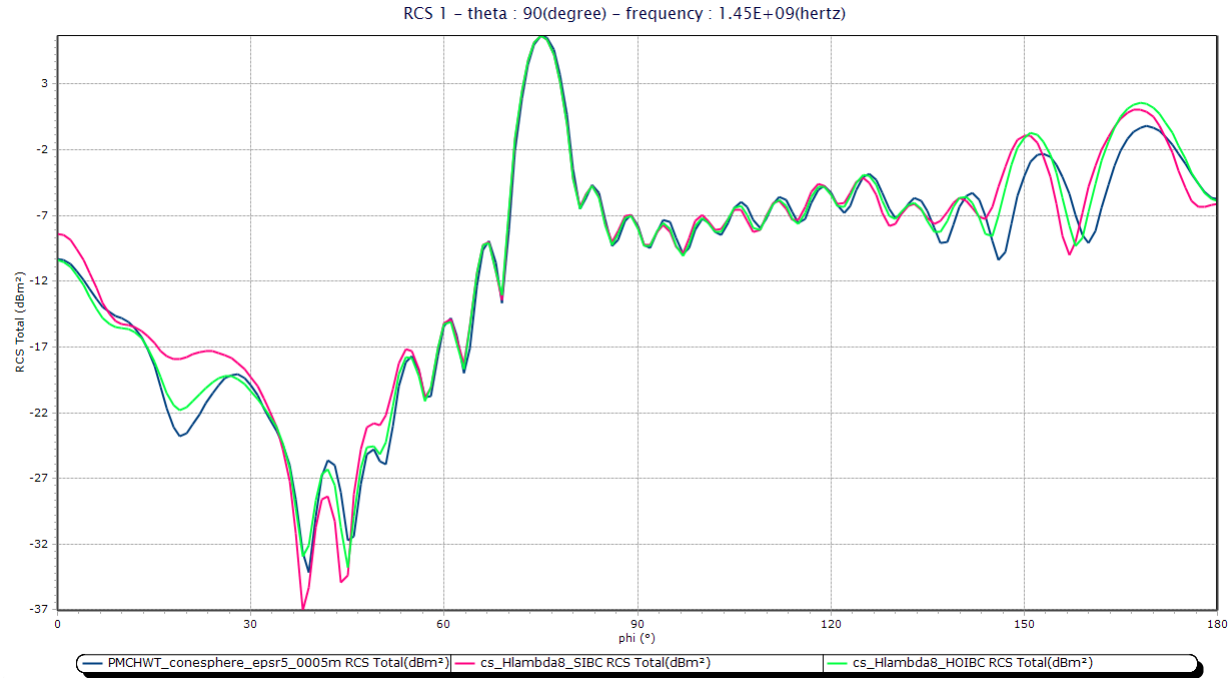

Figure 8: $\theta\theta$ component of the monostatic RCS for a coated conducting cone-sphere, PMCHWT solution and HOIBC solution.

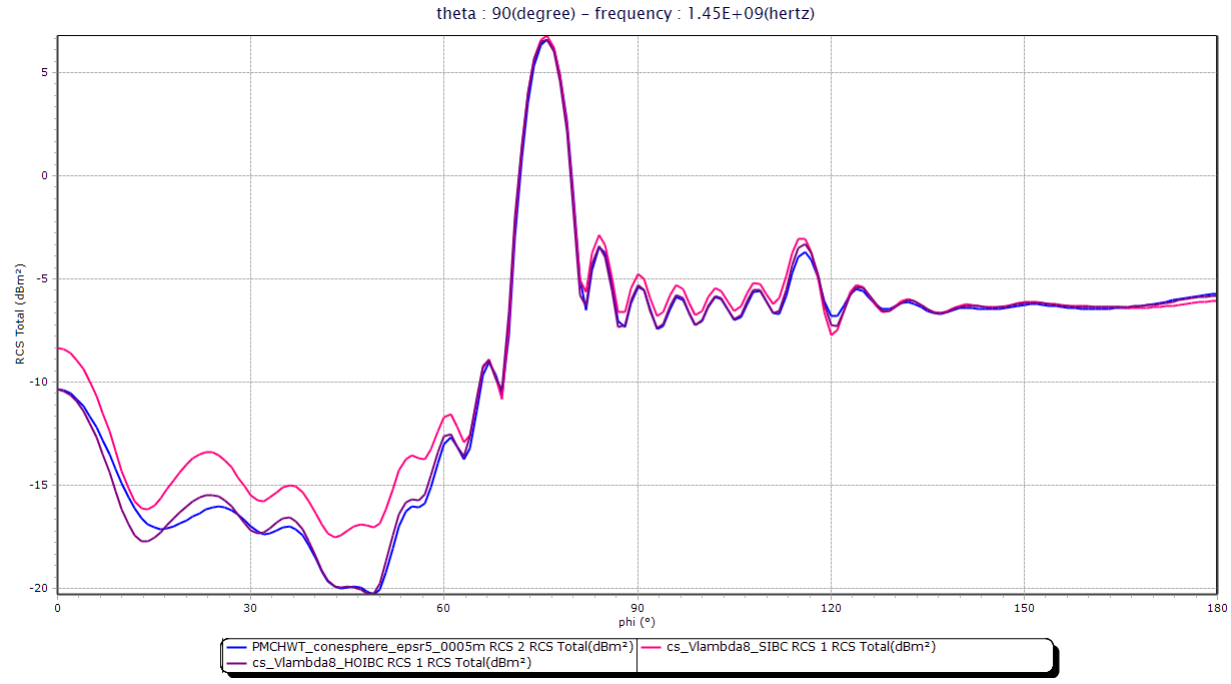

Figure 9: $\phi\phi$ component of the monostatic RCS for a coated conducting cone-sphere, PMCHWT solution and HOIBC solution.

Figure 8 and Figure 9 show the $\theta\theta$ and $\phi\phi$ components of the monostatic RCS. Three solutions are included : a method of moments solution called PMCHWT, the

HOIBC solution and the SIBC solution. Note that the HOIBC solution is much more accurate than the SIBC solution.

6 Coated cone

Our next concern is to assess the performance of our approximation HOIBC in this case the highest index coating. We consider a coated conducting cone which is illustrated in Figure 10. This PEC cone of total length 2 cm, tip radius 10 cm, diameter flat base 20 cm is coated with a 5cm layer, $\epsilon_r = 2 - 3i$ and $\mu_r = 1 - i$.

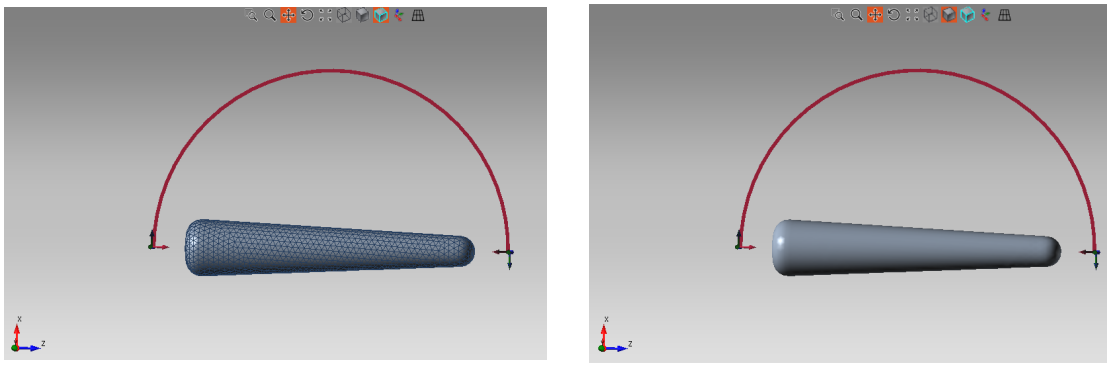

Figure 10: A mesh (right) and corresponding cone (left).

As can be seen in the Figure 11 and Figure 12 we present $\theta\theta$ and $\phi\phi$ of the monostatic RCS. Here, we compare the results obtained using HOIBC solution with various meshes and PMCHWT solution where the step is $h = \lambda_0/28$. For the highest index coating, the HOIBC solution is the most accurate.

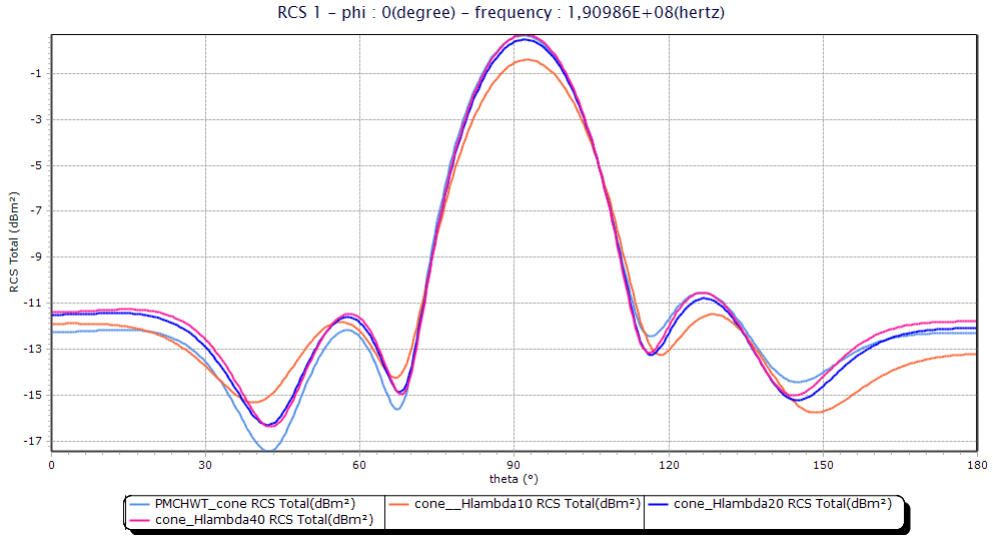

Figure 11: $\theta\theta$ component of the monostatic RCS for a coated conducting cone, PMCHWT solution and HOIBC solutions.

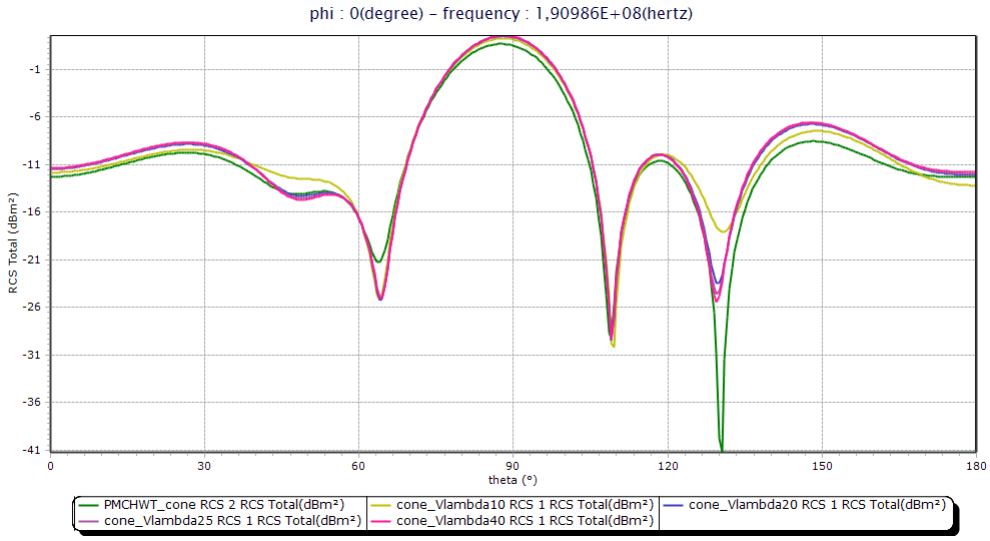

Figure 12: $\phi\phi$ component of the monostatic RCS for a coated conducting cone, PMCHWT solution and HOIBC solutions.

6.1 Coated cylinder

The next example, we consider a coated conducting cylinder which is illustrated in Figure 13. This PEC cylinder of total length 2m, hemisphere radius 25 cm, hemisphere radius 25 cm is coated with a 5 cm layer, $\epsilon_r = 1 - i$ and $\mu_r = 1$.

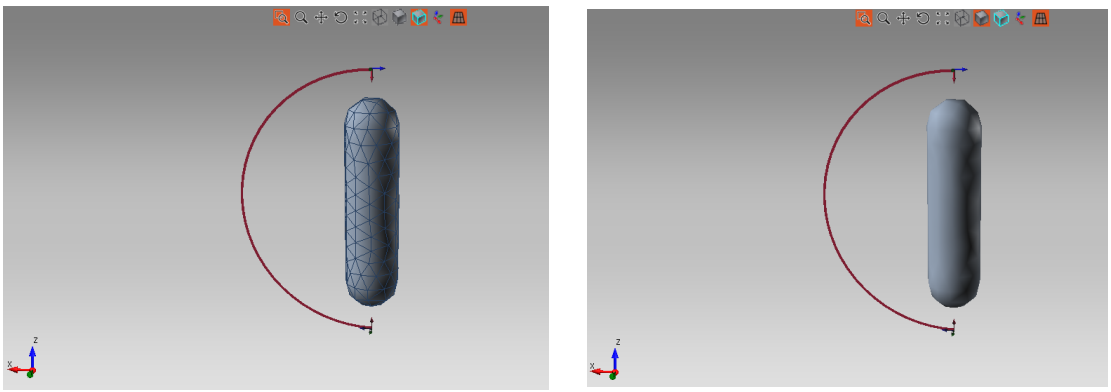

Figure 13: A mesh (right) and corresponding cylinder (left).

As in the previous test examples, we use the approximation HOIBC to compute these solutions for different values of h namely, $h = \lambda_0/10$, $h = \lambda_0/20$, $h = \lambda_0/25$, $h = \lambda_0/40$ while the step $h = \lambda_0/28$ to compute PMCHWT solution. The corresponding results for $\theta\theta$ and $\phi\phi$ components of monostatic RCS are presented in Figure 14 and Figure 15.

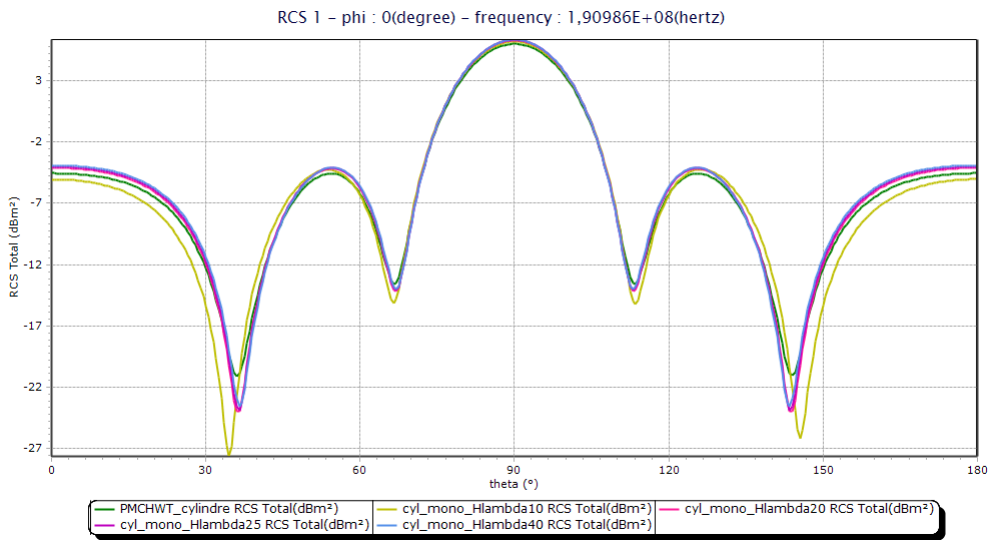

Figure 14: $\theta\theta$ component of the monostatic RCS for a coated conducting cylinder, PMCHWT solution and HOIBC solutions.

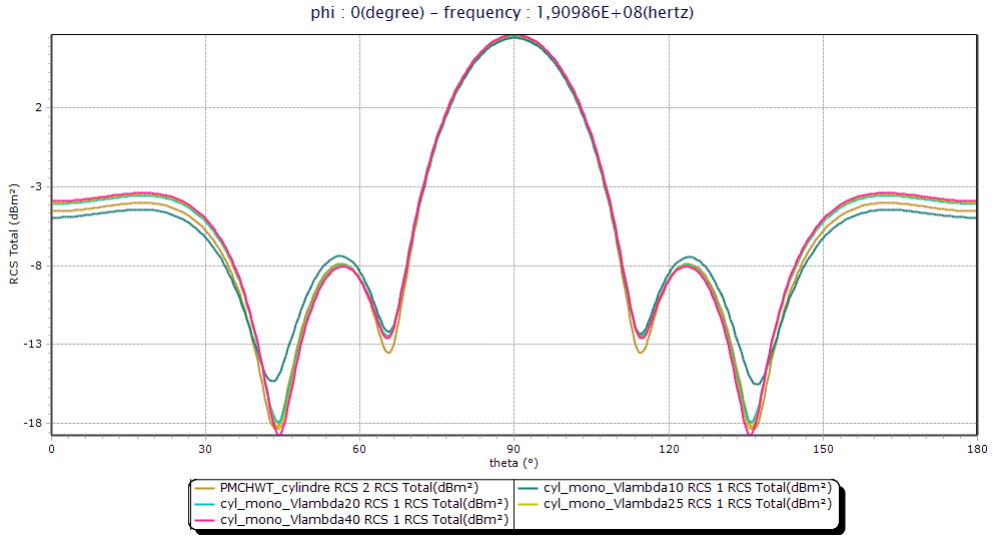

Figure 15: $\phi\phi$ component of the monostatic RCS for a coated conducting cylinder, PMCHWT solution and HOIBC solutions.

6.2 Coated Nasa Almond

As a final example, we consider a coated conducting nasa almond which is illustrated in Figure 16. From a numerical point of view this test example is more difiňĄcult than these previous. This PEC nasa almond of total length 2.56 m is coated with a 30mm layer, coating thickness of $0.1\lambda_0$, $\epsilon_r = 4$ and $\mu_r = 1$.

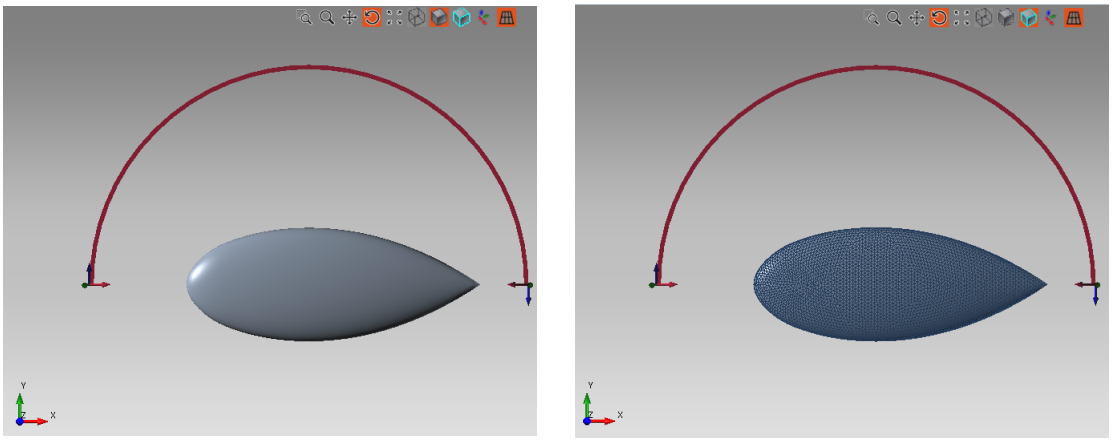

Figure 16: A mesh (right) and corresponding almond (left).

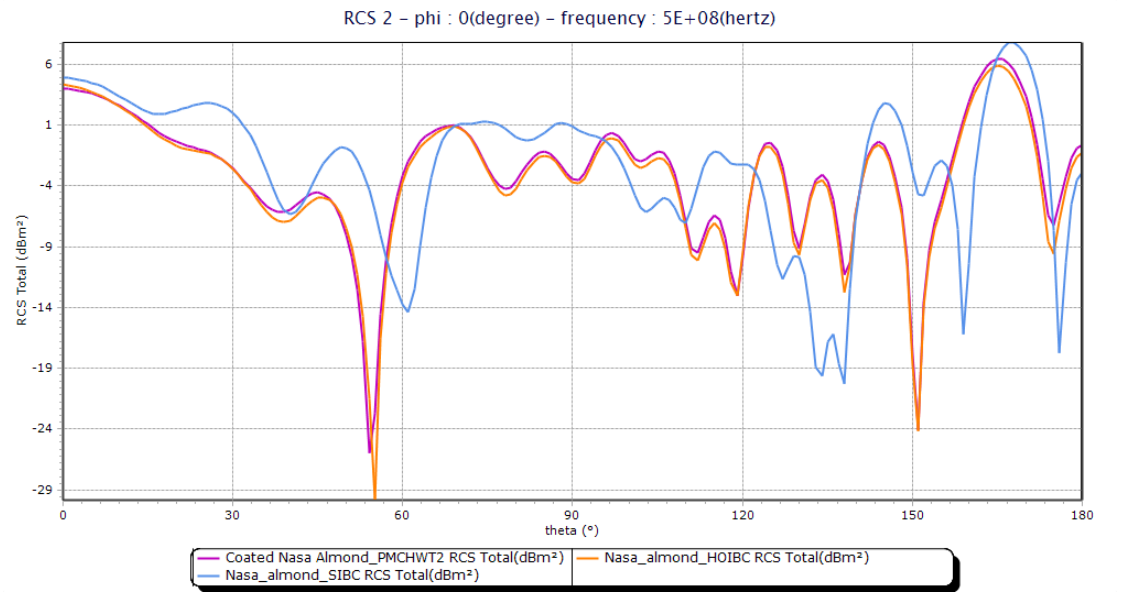

Figure 17: $\phi\phi$ component of the monostatic RCS for a coated conducting almond, PMCHWT solution, SIBC solution and HOIBC solution.

Figure 17 show the $\phi\phi$ components of the monostatic RCS. Three solutions are included : a method of moments solution called PMCHWT, the HOIBC solution and the SIBC solution. In the case clearly show the increased accuracy of the HOIBC solution relative to the SIBC solution. Moreover the approximation HOIBC that considers gives essentially the PMCHWT solution in all directions.

Then, the comparison of the calculation time is given by the following table:

Table 1: Computation time.

	Unknowns	Direct solve time (s on 16 cores)	ACA solve time (s on 16 cores)
Thick model	206514	48664	13284
SIBC model	29016	212	58
HIOBC model	29016	438	101

7 Conclusion

This paper proposed a new formulation of the electromagnetic scattering problem with a higher order impedance boundary condition which is an approximation of the relationship between the tangential traces of electric and magnetic fields . We proved the existence and uniqueness of the solution of the variational formulation which is a saddle point formulation. Then we discretized the formulation where J and M are the unknowns with Rao Wilson Glisson basis functions which are H(div). The numerical validations showed an important improvement in accuracy using the higher order impedance boundary condition over the standard impedance boundary condition model in the case of coated body and complex numerical simulations such as a coated conesphere and coated Nasa Almond validate the method.

ACKNOWLEDGMENT

The authors like to thank Nexio for allowing them to use CAPITOLE software.

References

[1] J. S. Asvestas, *Scattering by an indentation satisfying a dyadic impedance boundary condition*, *IEEE Trans. Antennas Propagat*, vol. 45, pp. 28âĂŞ33, Jan (1997).

[2] A. Bendali and K. Lemrabet, *The effect of a thin coating on the scattering of a time-harmonic wave for the Helmholtz equation*, *SIAM J. Appl. Math.*,pp. 1664-1693,(1996).

[3] Y. Rahmat-Samii and J. H. Daniel, *Scattering by Superquadric Dielectric-Coated Cylinders Using Higher Order Impedance Boundary Conditions*, *IEEE Trans. Antennas Propagat.*,vol. 40,No. 12,pp. 1513-1522, Dec (1992).

[4] B. Stupfel, *Impedance Boundary Conditions for Finite Planar or Curved Frequency Selective Surfaces Embedded in Dielectric Layers*, *IEEE Trans. Antennas Propagat*,Vol. 53,pp. 3654–3662,Nov (2005).

[5] B. Stupfel and O. Marceaux, *High-Order Impedance Boundary Conditions for Multilayer Coated 3-D Objects IEEE TRANSACTIONS ON ANTENNAS AND PROPAGATION*, Vol. 48,N. 3 pp. 429-436, March(2000).

[6] B. Stupfel and Y. Pion, *Impedance Boundary Conditions for Finite Planar or Curved Frequency Selective Surfaces*, *IEEE Trans. Antennas Propagat*,Vol. 53,pp. 1415–1424,April (2005).

[7] B. Stupfel, D. Poget and J. C. NÃľdÃľlec, *Sufficient uniqueness conditions for the solution of the time harmonic Maxwell's equations associated with surface impedance boundary conditions*, Journal of Computational Physics,Vol. 230, No 12,pp. 4571–4587, (2011).

[8] B. Stupfel, *One-way domain decomposition method with adaptive absorbing boundary condition for the solution of Maxwell's equations*, IEEE Trans. Antennas Propagat, Vol. 61, NO. 10,pp. 5100–5108, Aug (2015).

[9] G. C. Hsiao and R. F. Kleinman, *Mathematical foundations for error estimations in numerical solutions of integral equations in electromagnetics*, IEEE Trans. Antennas Propagat, vol. 45, pp. 316–328, Mar (1997).

[10] S. M. Rytov, *Calcul du skin-effet par la mÃľthode des perturbations*, J. Phys. USSR,Vol. 2,pp. 233–242, Oct (1940).

[11] J. G. Van Bladel, *Electromagnetic Fields*, Wiley, Second, (2007).

[12] A. Bendali, M. Fares and J. Gay, *A Boundary-Element Solution of the Leontovich Problem*, IEEE Trans. Antennas Propagat., Vol. 47, pp. 1597–1605, October, (1999).

[13] J. C. NÃľdÃľlec, *Acoustic and electromagnetic equations: Integral representations for harmonic problems*, Springer Ãľdition, Vol. 144, (2000).

[14] V. Lange, *Equations intÃľgrales espace-temps pour les Ãľquations de Maxwell: calcul du champ diffractÃľ par un obstacle dissipatif*, PhD thesis, MathÃľmatiques appliquÃľes, Bordeaux 1, (1995).

[15] C. Daveau and J. Laminie, *Mixed and Hybrid Formulations For The Three-Dimensional Magnetic Problem*, Numerical Methods for Partial Differential Equations, vol. 18, no. 1, pp. 85-104, January,(2002).

[16] S. M. Rao,D. R. Wilton and A. W. Glisson, *Electromagnetic scattering by surfaces of arbitrary shapes*, IEEE Trans. Antennas Propag, Vol. 30, No. 3, pp. 409–418, (1982).

[17] A. W. Glisson, *Electromagnetic scattering by arbitrary shapes surfaces with impedance boundary conditions*, Radio Sci, Vol. 27, No. 6, pp. 935–943, May, (1992).

[18] J. Jin, *The Finite Element Method in Electromagnetics*, New York: Wiley, (1993).

[19] S. N. Karp and F. C. Karal Jr, *Generalized impedance boundary conditions with applications to surface wave structures*, Electromagnetic Wave Theory, J. Brown, Ed. New York: Pergamon, pp. 479–483, (1967).

[20] T. B. A. Senior and J. L. Volakis, *Approximate boundary conditions in electromagnetics*, Inst. Elect. Eng. Electromagn. Waves Series 41, (1995).

[21] A. Aubakirov, *Electromagnetic scattering problem with hight order impedance boundary condition and integral methods*, *PHD Thesis*, Applied Mathematics, University of Cergy-Pontoise, January (2014).

[22] A. Bendali, *Numerical analysis of the exterior boundary value problem for the time-harmonic Maxwell equations by a boundary finite-element method, Part 2: The discrete problem*, Math. Comput., vol. 43, pp.47-68, (1984).

[23] P. L. Huddleston and Wang D. S., *An impedance boundary condition approach to radiation by uniformly coated antennas*, Radio Sci., vol. 24, pp. 427-432, (1989).

[24] Medgyiesi-Metschang, L. N., Putnam J.M. and Gedera M. B., *Generalized method of moments for three-dimensional penetrable scatterers*, *J. Opt. Soc. Am. A* , Vol. 11,No. 4, (1994).

[25] Y. Rahmat-Samii and J.H. Daniel, *Impedance Boundary Conditions in Electromagnetics*, *Taylor & Francis*, (1995).

[26] J. R. Rogers, *Moment method scattering solutions to impedance boundary condition integral equations*, *IEEE AP-S Int. Symp., Boston, MA*, pp. 347–350, (1984).

[27] G. C. Hsiao and R. F. Kleinman, *Mathematical foundations for error estimations in numerical solutions of integral equations in electromagnetics* , *IEEE Trans. Antennas Propagat.*, vol.45, pp.316-328, Mar.(1997).

[28] M. C ESSENAT, *Mathematical Methods in Electromagnetism*, *Mathematics for Applied Sciences, World Scientific*, Springer, vol. 41 (1996).

[29] T. B. A. Senior, *Impedance boundary conditions for imperfectly conducting surfaces Appl. Sci. Res., Section B*, vol. 8, pp. 418–436, (1960).

[30] M. N. Vouvakis, K. Zhao, S. M. Seo, and J. F. Lee, *A domain decomposition approach for non-conformal couplings between finite and boundary elements for unbounded electromagnetic problems in R3*, *J. Comput. Phys.*, vol. 225, pp. 975–994, (2007)

[31] C. A. Brebbia, J. C. F. Telles, and L. C. Wrobel, *Boundary Element Techniques*, *Theory and Application in Engineering, Springer-Verlag*, (1984).

[32] W. Hackbusch, *A sparse matrix arithmetic based on H-matrices. Part I: Introduction to H-matrices*, *Computing*, 62(2):89âĂŞ108 (1999).

[33] L. Grasedyck and W. Hackbusch, *Construction and arithmetics of H-matrices*, *Computing*, vol. 70, pp. 295âĂŞ334 (2003).

[34] A. Ida, T. Iwashita, T. Mifune and Y. Takahashi, *Parallel Hierarchical Matrices with Adaptive Cross Approximation on Symmetric Multiprocessing Clusters*, *JIP*, vol. 22, 642-650 (2014).

[35] T. Iwashita, Takeshi, A. Ida, T. Mifune, and Y. Takahashi, *Software Framework for Parallel BEM Analyses with H-matrices Using MPI and OpenMP*, *Procedia Computer Science*, 108:2200-2209 (2017).

[36] M. Bebendorf, *Approximation of boundary element matrices*, *Numer. Math*, vol. 86, pp. 565âĂŞ589 (2000).

[37] K. Zhao, M.N. Vouvakis, and J. Lee, *The Adaptive Cross Approximation Algorithm for Accelerated Method of Moments Computations of EMC Problems*, *Electromagnetic Compatibility, IEEE Transactions on*, 47. 763-773 (2005).